LBL-18778

Lawrence Berkeley Laboratory

UNIVERSITY OF CALIFORNIA

Materials & Molecular Research Division

Presented at the International Symposium on
Americium and Curium Chemistry and Technology,
1984 International Chemical Congress of Pacific
Basin Societies, Honolulu, HI,
December 16-21, 1984

THE ELECTRONIC AND MAGNETIC PROPERTIES OF Am AND Cm

N. Edelstein

LBL--18778

DE85 008512

February 1985

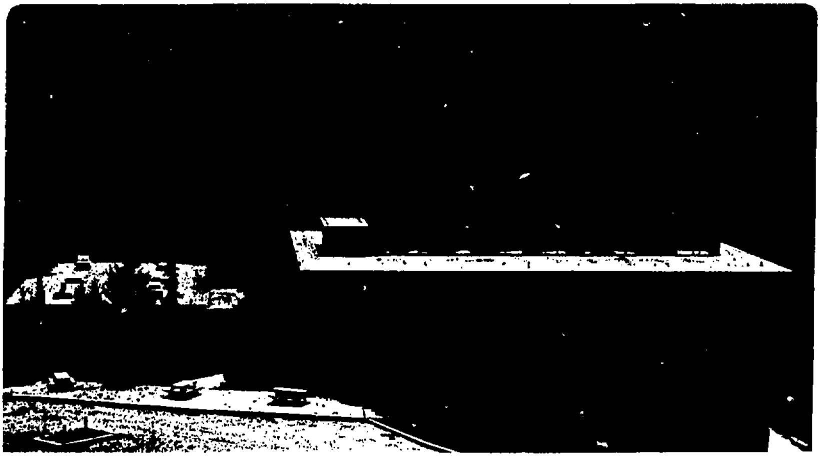

Prepared for the U.S. Department of Energy under Contract DE-AC03-76SF00098

LBL-18778

THE ELECTRONIC AND MAGNETIC PROPERTIES OF Am AND Cm

Norman Edelstein
Materials and Molecular Research Division
Lawrence Berkeley Laboratory
University of California
Berkeley, California 94720 U.S.A.

ABSTRACT. A review of the present status of the analyses of the optical spectra of Am and Cm in various oxidation states will be given. From these analyses, the magnetic properties of the ground states of these ions can be determined. These predicted values will be compared with the various magnetic measurements available.

1. INTRODUCTION

The optical and magnetic properties of Am and Cm have now been studied for over 30 years. The common oxidation state for these elements is the trivalent one, and their lanthanide analogues in this oxidation state have magnetic properties which differ from the rest of the lanthanide series. This fact has made the study of the magnetic properties of the Am^{3+} and Cm^{3+} ions of special interest in order that the differences (or similarities) between the 4f and 5f series could be determined. In this paper the optical properties of the various accessible oxidation states of these two elements will be briefly reviewed, followed by a review of their magnetic properties. The optical properties of the atoms in the gaseous phase or as free ions will not be covered.

2. Optical Spectra

The optical spectra for AmX_3 (X = $C\ell$, Br, I) and Am^{3+} and Cm^{3+} in single crystals of $LaC\ell_3$ have been measured and analyzed [1-4]. The free ion energy levels of Cm^{3+} (aquo) have also been assigned on the basis of the correlation between observed and calculated band intensities [5]. Other oxidation states of both Am (divalent, tetravalent to hexavalent) and Cm (tetravalent) are known and low resolution spectra of the tetravalent state in solids and solution have been obtained [6-9]. Recently, calculated free ion spectra for Am^{4+} and Am^{2+} have been published [10]. Selective laser excitation experiments on Cm^{3+} in D_2O have also been carried out [11].

3. Magnetic Properties

Magnetic properties of materials determined by bulk magnetic susceptibility or electron paramagnetic resonance (epr) measurements are usually determined by the energy levels of the materials which are populated at the temperatures of the measurement. Most epr spectra of actinide ions are measured at 4.2 K so usually only the magnetic properties of the ground crystal field state are determined. Magnetic susceptibility measurements are performed in a range of temperatures (~2-300 K) so the splittings of lowest J level may sometimes be determined [12,13]. If the ground state is a singlet (non-magnetic), the magnetism of the material is determined by the mixing of the higher lying magnetic states into the ground state by the magnetic field. This type of magnetic behavior is independent of temperature (if the magnetic state lies much higher than kT). Table 1 lists the configurations of various oxidation states of Am and Cm for which magnetic data have been measured. Each of these configurations will be discussed individually.

4. $5f^5$ - Am^{4+}

The ground term for the Am^{4+} ion is a nominally $^6H_{5/2}$. However because of the strong spin-orbit coupling for actinide ions, this state is less than 66% pure. This number comes from calculations on Pu^{3+} [14]. Table 2 shows the eigenvector components for Sm^{3+} and Pu^{3+} free ions. Am^{4+} has a larger spin-orbit coupling constant than Pu^{3+}, thus the Pu^{3+} eigenvector represents a lower limit for an Am^{4+} intermediate-coupled

Table 1. Accessible Oxidation State for Am and Cm

	Am	Cm	Ground State
$5f^5$	Am^{4+}	-	J = 5/2
$5f^6$	Am^{3+}	Cm^{4+}	J = 0
$5f^7$	Am^{2+}	Cm^{3+}	J = 7/2

Table 2. Largest Eigenvector Components for Sm^{3+} and Pu^{3+} Ground J = 5/2 State (Ref. 14)

Sm^{3+}

$96.0\%\ {}^6H + 2.3\%\ {}^4G4 + 1.4\%\ {}^4G1 + \cdots.$

Pu^{3+}

$66.0\%\ {}^6H + 14.3\%\ {}^4G4 + 9.6\%\ {}^4G1 + 1.7\%\ {}^4F3 + 1.2\%\ {}^4G3 + 1.0\%\ {}^2F6$
$+ 1.0\%\ {}^6F + 1.0\%\ {}^2F2 + \cdots.$

eigenvector. Since most of the calculations have been done for Pu^{3+} systems, these will be summarized, but the same arguments hold for Am^{4+} in sites of the same symmetry.

Electron paramagnetic resonance has been reported for Am^{4+} diluted in ThO_2 and CeO_2 single crystals [15,16]. The site symmetry for the Am^{4+} ion is cubic. For a J = 5/2 state in cubic symmetry the crystal field will split this term into two states, a Γ_7 doublet and Γ_8 quartet state. For this symmetry the splitting of these two levels depends on two crystal field parameters B_0^4 and B_0^6, and angular factors which depend on the intermediate coupled wavefunction. These angular factors have been calculated for Sm^{3+} and Pu^{3+}, and it has been shown that the sign of B_0^4 (which is the dominant term) for Pu^{3+} (or Am^{4+}) is opposite to that for Sm^{3+} [14]. This sign change is due to the large admixture of higher L-S states by the spin-orbit coupling interaction. The net result is that for Sm^{3+} the Γ_8 state would be lowest, but for Pu^{3+} or Am^{4+}, the Γ_7 state is the ground state. This is illustrated in Fig. 1.

For an isolated Γ_7 state the calculated g value should be equal to

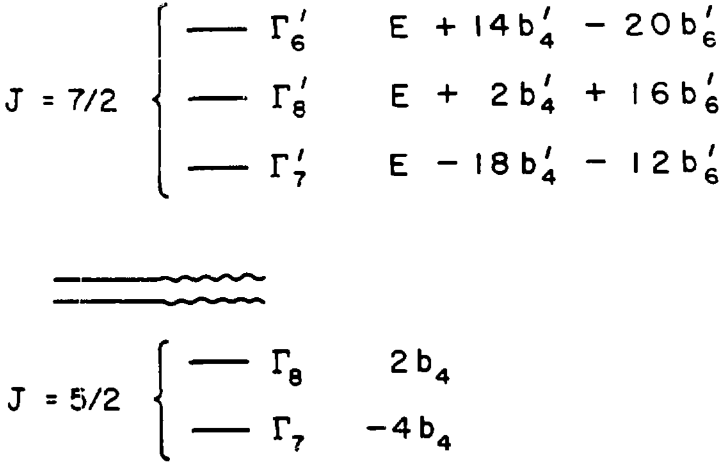

Figure 1. Schematic energy level diagram for Pu^{3+}/CaF_2 and Am^{4+}/ThO_2, CeO_2. For Sm^{3+} (the 4f analogue), the Γ_7 and Γ_8 energy level ordering for the ground J = 5/2 state is reversed.

-0.700. The measured values for Am^{4+} in CeO_2 and ThO_2 are as shown in Table 3. Note that these two values are different with Am^{4+}/ThO_2 being larger. For Pu^{3+} the first excited state is a J=7/2 which is calculated to be at ~3200 cm^{-1}. In the actinide series, crystal field

Table 3. Measured g values for $5f^5$ Ions in Various Hosts (Ref. 16)

		|A| (10^{-4} cm^{-1})		B_4'[a]
Matrix	|g|	$^{239}Pu^{3+}$	$^{241}Pu^{3+}$	(cm^{-1})
CeO_2	1.333 ± 0.001	22.4 ± 0.2		-5400
ThO_2	1.3124 ± 0.0005	65.4 ± 0.2		-5130
			46.1 ± 0.6	
CaF_2	1.297 ± 0.002	66.95 ± 0.03		-4945
			48.07 ± 0.10	
SrF_2	1.250 ± 0.002	84.6 ± 1.0		-4440
BaF_2	1.187 ± 0.004	102 ± 3		-3820
$SrCl_2$	1.1208 ± 0.0005	127.9 ± 0.4		-3190

		|A| (10^{-4} cm^{-1})	
Matrix	|g|	$^{241}Am^{4+}$	$^{243}Am^{4+}$
CeO_2	1.3120 ± 0.0005		22.1 ± 0.2
ThO_2	1.2862 ± 0.0005	45.7 ± 0.1	45.3 ± 0.1

---

[a] Values of B_4' were calculated assuming that $B_6'/B_4' = -0.2$.

effects are large and this interaction can mix excited states into the ground state. Using a model which considered only the mixing of these two states, Edelstein, et al. fit a series of g values for Pu^{3+} in CaF_2, SrF_2, and BaF_2 showing that the crystal field interaction decreased as the lattice parameter increased [14]. This same model has been applied to fit the g values for Am^{4+} in ThO_2 and CeO_2 [16]. The results are consistent with CeO_2 (the smaller lattice) having a larger crystalline field interaction at the Am^{4+} site than ThO_2. A plot of the g values vs. the crystal field parameter is shown in Fig. 2. A more complete

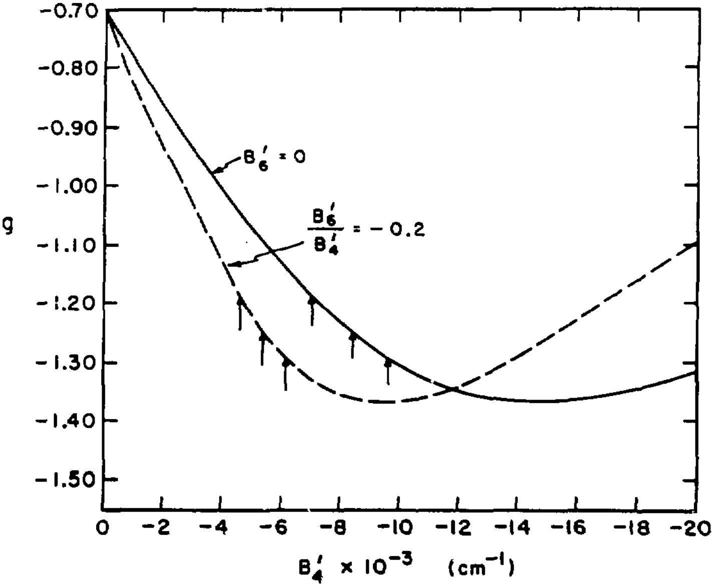

Figure 2. Plot of calculated g value vs. B_4'. The solid line describes the calculated values for $B_6' = 0$. The dotted line describes the values for $B_6'/B_4' = -0.2$. The arrows show where the experimental g values are located for Pu^{3+}/CaF_2, SrF_2, BaF_2. A similar plot may be drawn for Am^{4+}/CeO_2, ThO_2.

calculation for Pu^{3+} in cubic lattices has been given by Lam and Chan [17].

The magnetic susceptibility of $^{243}AmO_2$ as a function of temperature has been reported [18]. An antiferromagnetic transition was found at 8.5 ± 0.5 K. This transition was not found in a neutron diffraction study on $^{243}AmO_2$ at 20 K and 6.5 K nor was a hyperfine field detected for AmO_2 by a Mossbauer study [19]. The ground state g value of AmO_2 was found to be 1.51 which is 17% larger than for Am^{4+} in ThO_2, and the excited Γ_8 state was determined to be at ~35 K [18].

5. $5f^6$ - Am^{3+}, Cm^{4+}

The $5f^6$ configuration has a nominally $^7F_0$ ground term. Spin-orbit coupling will mix in other J = 0 states, but this state must be a singlet in all crystal fields. Consequently all magnetic effects will come from second order interactions and will result in temperature independent paramagnetism (TIP). The measured susceptibilities will be small in magnitude and impurities in the sample could drastically affect the measured values. With small radioactive samples (100 µg - 10 mg) containing the isotopes $^{241 \text{ or } 243}Am$ and $^{244 \text{ or } 248}Cm$, contamination of samples either with chemical impurities, or by radiation damage is a major problem. It is not surprising that the few results available vary greatly. If we assume the B_0^2 crystal field parameter does not change much from one compound to another (this is the only parameter which will split the J = 1 first excited state in compounds with C_3 or higher symmetry) then all Am^{3+} compounds should have about the same value for their temperature independent paramagnetism. Table 4 lists the values for a number of Am^{3+} compounds [20-25]. Am metal is the first actinide metal to exhibit a localized trivalent moment. Table 4 lists the magnetic susceptibility for Am, and whose value is in the range of trivalent Am compounds.

Cm^{4+} compounds show an anomalous temperature dependence [22,26-28]. Theoretically they should be similar to the Am^{3+} compounds and show

Table 4. Magnetic Susceptibility of Am^{3+} Compounds and Am Metal

Compound	TIP (10^{-6} emu/mole)	Reference
Am_2O_3	800 ± 200	20
$Cs_2NaAmCl_6$	5400 ± 400	21
AmF_3	714 ± 1%[a]	22
AmF_3	566 ± 25[b]	23
AmF_3	1040 ± 300[b]	24
Am^{3+} on bead	716 ± 100[b]	23
Am^{3+} in solution	720	25
Am metal	881 ± 46	23
Am metal	675	25a
Calculated	~500[c]	20

[a] Temperature dependent μ_{eff} = 0.63 BM.

[b] Slightly temperature dependent.

[c] From optical data on $Am^{3+}/LaCl_3$. The J=1 level is 2720 cm^{-1} above the ground J=0 level.

temperature independent paramagnetism. However they are temperature dependent and have effective magnetic moments between 2-4 Bohr magnetons. Kanellakopolus has followed the magnetic susceptibility of a $^{244}CmO_2$ sample as function of time and found the magnetism increases linearly [26]. He proposed that this increase was due to the formation of Cm^{3+} (a $5f^7$ ion with μ_{eff} ~ 7.9 BM) caused by the radiation damage due to the alpha particles from the decay of ^{244}Cm nuclei. He was able to fit his data by assuming a rate of production of Cm^{3+} of 2.09% per month. Goffart found a similar time dependence in his magnetic measurements on $^{244}CmO_2$ [27]. Presumably compounds synthesized with

^{248}Cm ($\tau_{1/2}$ = 4.7 x 10^5y compared with $\tau_{1/2}$ = 18.1y for ^{244}Cm) should be much less sensitive to these effects. Hurray et al. have reported temperature dependent behavior for various $^{248}Cm^{4+}$ compounds. Goffart et al. and Morss et al. also found temperature dependent behavior for $^{248}CmO_2$ [27,28]. The lattice constants of these samples obtained by x-ray powder diffraction techniques showed no indication of an expanded structure [27,28]. Further studies are necessary for the Cm^{4+} compounds.

6. $5f^7$, Am^{2+}, Cm^{3+}

The half-filled shell configuration, $4f^7$, in the lanthanide series gives a ground state wavefunction for Gd^{3+} which is approximately 98% $^8S_{7/2}$ (see Table 5). This state will not be split by the crystalline field.

Table 5. Leading Terms in the Wavefunctions for Gd^{3+} and Cm^{3+},

J = 7/2 (Ref. 35)

Gd^{3+}

$97.4\%\ ^8S + 2.6\%\ ^6P + .01\%\ ^6D + \cdots$

Cm^{3+}

$79.4\%\ ^8S + 17.1\%\ ^6P + .81\%\ ^6D + \cdots.$

Nevertheless from epr measurements, splittings on the order of .1 to 1 cm^{-1} are observed for Gd^{3+} in various crystalline environments. These splittings arise from various higher order mechanisms which have been proposed [29]. The first report of the epr of Cm^{3+} was made by a group at Berkeley who found a group of seven lines at 4.2 K in $^{244}Cm^{3+}/LaCl_3$ characteristic of a $J = 7/2$ level with $g = 1.991$ [30]. This observation was confirmed by a group at Argonne National Laboratory [31]. The ground state of Cm^{3+} was supposed to be analogous to its $4f^7$ counterpart Gd^{3+}, and these data confirmed this similarity.

As more information became available about the electronic structure of the actinides, it became increasingly clear something was wrong with the above observations. The AmI $(5f^7 7s^2)$ g value was measured by atomic beam methods, and it was found to be 1.937 [32]. Runciman [33] obtained wavefunctions for Cm^{3+} and from these wavefunctions the g value of the ground state was calculated to be 1.913 [34]. These deviations from $g = 2.00$ were due to the large extent of intermediate coupling for Cm^{3+}. Abraham, Judd, and Wickman [34] reexamined the $Cm^{3+}/LaCl_3$ epr spectrum and found a strong single line with $g_{||} = 1.925 \pm 0.002$ and $g = 7.67 \pm 0.02$. A similar spectrum was found for Cm^{3+} diluted in lanthanum ethylsulfate. These spectra were readily explained on the basis of the zero field splitting for Cm^{3+} being large with respect to the microwave frequency. Thus the initial reports were spurious and the Cm^{3+} epr spectrum was consistent with other actinide data and theory.

The leading terms in the wave functions for Cm^{3+} and Gd^{3+} are shown in Table 5. Cm^{3+} is only about 79% pure $^8S_{7/2}$. The three leading terms will not split in a cubic crystalline field. An approximate calculation using the complete 50 term wavefunction for Cm^{3+} showed qualitatively that the effects of intermediate coupling can account for the much larger splitting in Cm^{3+} than in its $4f^7$ counterpart, Gd^{3+}.

The crystal field splittings for Cm^{3+} in cubic compounds are of the order of 5-50 cm^{-1}. The ground state is an isotropic Γ_6 state and the first excited state is an anisotropic Γ_8 state. If the splitting between these two states is of the order of magnitude of the magnetic splittings, these two states can be mixed by the magnetic field in an epr experiment [35]. This will result in the ground Γ_6 state showing some anisotropy. From the magnitude of the anisotropy, the Γ_6-Γ_8 splittings can be deduced. Some of the results are shown in Table 6.

Table 6. Zero-field Splittings of the $5f^7$ Ions in Various Crystals (Ref. 36)

Crystal	Ion	(cm^{-1})	(cm^{-1})	g_J
$SrCl_2$	Cm^{3+}	5.13 ± 0.05	15.3 ± 0.4	1.928 ± 0.002
SrF_2	Cm^{3+}	11.2 ± 0.4		1.9257 ± 0.001
CaF_2	Cm^{3+}	13.4 ± 0.5		1.926 ± 0.001
ThO_2	Cm^{3+}	15.5 ± 0.3		1.9235 ± 0.002
$SrCl_2$	Am^{2+}	5.77 ± 0.48		1.9283 ± 0.0008
SrF_2	Am^{2+}	15.2 ± 0.4		1.9254 ± 0.001
CaF_2	Am^{2+}	18.6 ± 0.5		1.926 ± 0.001

For Cm^{3+} in $SrCl_2$, both the Γ_6 and the Γ_7 resonances were observed. Both were anisotropic as shown in Fig. 3. Both the $\Gamma_7 - \Gamma_8$ and $\Gamma_6 - \Gamma_8$ splittings for Cm^{3+} in $SrCl_2$ are shown in Table 6 [36]. Finally, in Table 7 the zero field splitting for Gd^{3+} and Cm^{3+} in a number of cubic crystals are listed [38]. Note that the splitting for Gd^{3+}/CeO_2 is smaller than for Gd^{3+}/ThO_2. Based on an electrostatic model one would expect the crystal field splitting to be inversely proportional to the lattice constant (for anions of the same charge). The higher order mechanisms must predominate for Gd^{3+} in ThO_2 and CeO_2. However for Cm^{3+} with its larger splitting the electrostatic mechanism appears to be the predominant one.

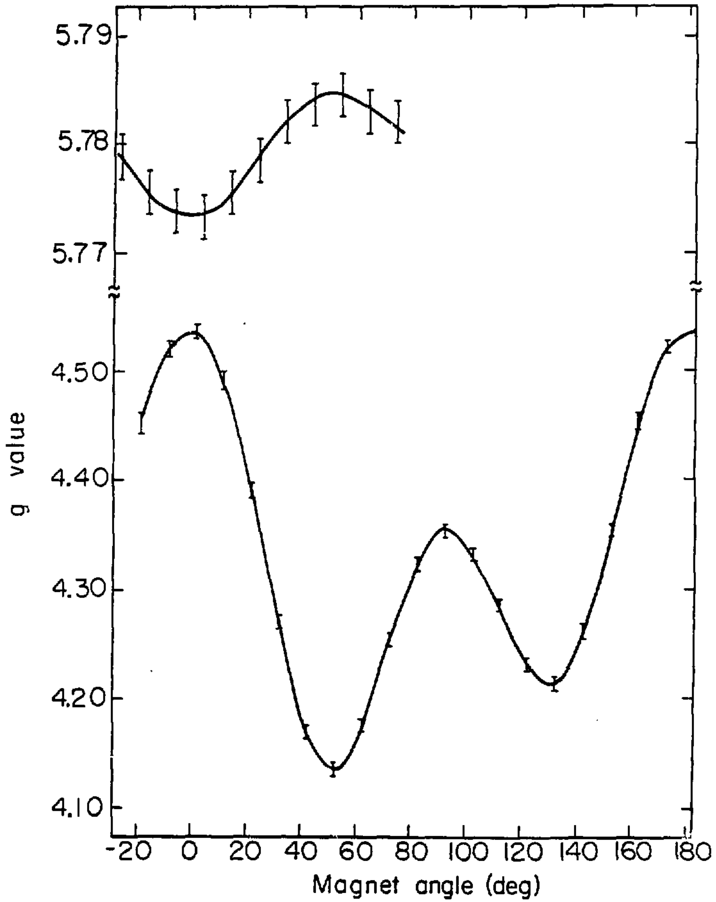

Figure 3. The measured g value as a function of the rotation of the dc magnetic field for $SrCl_2:Cm^{3+}$. The data were obtained at ~35 GHz and ~5500 G. The smooth curves are calculated values. Note the change in scale for the Γ_7 (upper curve) and Γ_6 (lower curve) states. The error bars for the Γ_6 state are ±0.005, for the Γ_7 state ±0.002.

Table 7. Zero-field Splittings for Gd^{3+} and Cm^{3+} in Various Host Crystals at 4.2 K (Ref. 37)

	Lattice Constant (A)	Gd^{3+} (cm^{-1})	Cm^{3+} (cm^{-1})
CeO_2	5.41	0.0653 ± 0.0004	17.8 ± 0.3
ThO_2	5.60	0.06645 ± 0.00008	15.5 ± 0.3
CaF_2	5.46	0.0578 ± 0.0001	13.4 ± 0.5
SrF_2	5.80	0.0501 ± 0.0002	11.2 ± 4
BaF_2	6.20	0.0448 ± 0.0002	-
$SrCl_2$	7.00	0.01979 ± 0.0004	5.13 ± 0.5

The epr spectra of Cm^{3+} in a number of tetragonal crystals have been reported [38,39]. In D_{2d} symmetry the crystal field states will have eigenfunctions of the type

$a| \pm 7/2\rangle + b| \mp 1/2\rangle$

or

$c| \pm 5/2\rangle + d| \mp 3/2\rangle$

From the measured g values the admixture coefficients may be evaluated and, from measurements at different temperatures, it can be determined if the state observed is the ground state. For the system $Cm^{3+}/ThSiO_4$, no epr spectrum was observed [40]. In the hosts for which both Cm^{3+} and Gd^{3+} epr signals have been observed, the dominant crystal field term has had the same sign. For $Gd^{3+}/ThSiO_4$, B_0^2 is the dominant term with a sign < 0. Assuming that $B_0^2 < 0$ and dominant for the $Cm^{3+}/ThSiO_4$ system, the state with $a|\pm 7/2\rangle + b|\mp 1/2\rangle$ would be the ground state with the values $a \sim 1$ and $b \sim 0$. Some recent data of the various crystal field levels for the tetragonal system $Cm^{3+}/LuPO_4$ are shown in Table 8. The g values measured at 77 K and 4.2 K are slightly different due to the change in the crystal field as a function of temperature. The net result of this change is a small difference in the energies and composition of the eigenvectors of the system as a function of temperature which is reflected in the g values. All the intensities of the epr lines for $Cm^{3+}/LuPO_4$ showed decreases as the temperature was lowered. This

Table 8. g Values for the Crystal Field Levels of $Cm^{3+}/LuPO_4$ (Ref. 39)

	Eigenvector	Calculated		Measured	
		$g_\parallel$	$g_\perp$	$g_\parallel$	$g_\perp$
77K	$0.9837\ |\pm 1/2\rangle - 0.1798\ |\mp 7/2\rangle$	1.424	7.436	1.424	7.436
	$0.9463\ |\pm 3/2\rangle - 0.3233\ |\mp 5/2\rangle$	4.155	4.07	4.15	4.07
	$0.9463\ |\pm 5/2\rangle + 0.3233\ |\mp 3/2\rangle$	8.0	4.07	8.0	4.07
	$0.9837\ |\pm 7/2\rangle + 0.1798\ |\mp 1/2\rangle$	12.95	0.25	-	-
4.2K	$0.98205\ |\pm 1/2\rangle - 0.1886\ |\mp 7/2\rangle$	1.373	7.402	1.373	7.402
	$0.9455\ |\pm 3/2\rangle - 0.3255\ |\mp 5/2\rangle$	4.13	4.096	4.12	4.10
	$0.9455\ |\pm 5/2\rangle + 0.3255\ |\mp 3/2\rangle$	7.976	4.086	7.98	4.096
	$0.98205\ |\pm 7/2\rangle + 0.1886\ |\mp 1/2\rangle$	12.9	0.27	-	-

observation may be explained by again assuming that $B_0^2 < 0$ and is the dominant term. Thus the state with $a = -1.0$ must be the ground state.

Magnetic susceptibility measurements for various trivalent Cm compounds and AmI_2 are shown in Table 9 [21,22,41-44]. For a free ion

Table 9. Summary of magnetic data for Cm compounds

Compound	T (K)	μ_{eff}[a] BM	θ (K)	References
$CmF_3 \cdot 1/2\ H_2O$	77-298	7.7	-5	41
CmOCl	77-298	7.6	-22	41
CmF_3 in LaF_3	77-298	7.7	-6	41
Cm^{3+} in	7.5-25	7.9	-4	21
$Cs_2NaLuCl_6$	25-45	7.5	-1	21
Cm_2O_3[b,c]	20-80	8.20	-149	42
	100-300	7.89	-130	42
CmN	140-300	7.02	+109	43
CmAs	100-300	6.58	+88	43
CmF_3	-30-280	7.67	3.6	22
Cm_2O_3[c]	50-300	7.74	-130	22
Cm_2O_3[d]	4.2-300	7.51	-110	22
AmI_2	37-180	6.7 ± .7	e	44

---

[a] $\mu_{eff} = 2.828\ (T-\theta)^{1/2}$ BM.

[b] Antiferromagnetic transition at $T = 13 \pm 2$ K.

[c] Monoclinic phase.

[d] bcc.

[e] not given in Ref. 44.

μ_{eff} = 7.9BM. Thus most of the data at high temperatures agree with the expected theoretical value. Cm metal exhibits a localized moment characteristic of rare earth metals and the heavier actinide metals (starting at Am). Various magnetic measurements have been made on Cm metal with ^{244}Cm and ^{248}Cm [45]. The values given vary widely, and these measurements should be repeated. A transition to an antiferromagnetic phase has been reported below 52 K [46].

7. Conclusion

The magnetic properties of the elements Am and Cm, and their compounds can be explained on the basis of the wavefunctions obtained from optical spectra or from wavefunctions obtained from extrapolated parameters. For Cm^{4+} data the experimental data show an anomalous temperature dependence. Further work is needed on these compounds. There is a large scatter in the data for Cm metal, and this system should also be reexamined.

8. Acknowledgements

I would like to thank M.M. Abraham and L. Boatner for allowing me to quote their Cm^{3+} data before publication, and L. Soderholm and L.R. Morss for helpful comments about the manuscript. This work was supported by the Director, Office of Energy Research, Office of Basic Energy Sciences, Chemical Sciences Diviso: of the U.S. Department of Energy under Contract No. DE-AC03-76SF00098.

References

1. R.G. Pappalardo, W.T. Carnall, and P.R. Fields, J. Chem. Phys. 51, 1182 (1969).
2. J.G. Conway, J. Chem. Phys. 40, 2504 (1964).
3. J.B. Gruber, W.R. Cochran, J.G. Conway, and A.T. Nicol, J. Chem. Phys. 45, 1423 (1966).

4. J.P. Hessler and W.T. Carnall, in "Lanthanide and Actinide Chemistry and Spectroscopy," N. Edelstein, Ed., ACS Symposium Sseries 131, 349 (1980).
5. W.T. Carnall and K. Rajnak, J. Chem. Phys. 63, 3510 (1975).
6. T.K. Keenan, J. Am. Chem. Soc. 83, 3719 (1961).
7. L.B. Asprey and T.K. Keenan, J. Inorg. Nucl. Chem. 7, 27 (1958).
8. F.H. Krause and L.B. Asprey, Inorg. Chem. 1, 137 (1962).
9. L.B. Asprey and R.A. Penneman, Inorg. Chem. 1, 134 (1962).
10. J. Blaise, M.S. Fred, W.T. Carnall, H.M. Crosswhite, and H. Crosswhite in "Plutonium Chemistry," W.T. Carnall and G.R. Choppin, Eds., ACS Symposium Series 216, 173 (1983).
11. J.V. Beitz and J.P. Hessler, Nucl. Tech 51, 169 (1980).
12. For a comprehensive review of the epr of actinide ions see L.A. Boatner and M.M. Abraham Repts. Prog. Phys. 41, 87 (1978).
13. A review of the magnetic properties of the actinides is given by N. Edelstein and J. Goffart, "Magnetic Properties of the Actinides," in "Chemistry of the Actinide Elements," J.J. Katz, G.T. Seaborg, and L. Morss, Eds., Chapman and Hall, London, in press.
14. N. Edelstein, H.F. Mollet, W.C. Easley, and R.J. Mehlhorn, J. Chem. Phys. 51, 3281 (1969).
15. M.M. Abraham, L.A. Boatner, C.B. Finch, and R.W. Reynolds, Phys. Rev. B 3, 2864 (1971).
16. W. Kolbe, N. Edelstein, C.B. Finch, and M.M. Abraham, J. Chem. Phys. 60, 607 (1974).
17. D.J. Lam and S.K. Chan, Phys. Rev. B 6, 307 (1972).
18. D.G. Karraker, J. Chem. Phys. 63, 3174 (1975).
19. A. Boeuf, J.M. Fournier, J.F. Guegnon, L. Manes, J. Rebizant, and F. Rustichelli, J. Phys. Lett. 40, 335 (1979).
20. L.R. Morss, G. Shalimoff, and N. Edelstein, (to be published).
21. M.E. Hendricks, E.R. Jones, Jr., J.A. Stone, and D.G. Karraker, J. Chem. Phys. 60, 2095 (1974).
22. S.E. Nave, R.G. Haire, and P.G. Huray, Phys. Rev. B 28, 2317 (1983).
23. D.B. McWhan, Ph.D. thesis, UCRL-9695, 1961.

24. W.W.T. Crane, J.C. Wallmann, and B.B. Cunningham, UCRL-846, 1950.

25. J.J. Howland, Jr. and M. Calvin, J. Chem. Phys. 18, 239 (1950).

25a. W.J. Nellis and M.B. Brodsky, in "The Actinides: Electronic Structure and Related Properties, Vol. II," A.J. Freeman and J.B. Darby, Jr. Eds., Academic Press, New York, 1974, p. 266.

26. B. Kanellakopulos, "Magnetochemie," Lecture at the Institut für Radiochemie der Technischen Universität München, 1979.

27. J. Goffart, unpublished work, 1982.

28. L.R. Morss, E. Gamp, and N. Edelstein, unpublished work, 1983.

29. V.M. Malhotra and H.A. Buckmaster, Canad. J. Phys. 60, 1573 (1982) and references therein.

30. M. Abraham, B.B. Cunningham, C.D. Jeffries, R.W. Kedzie, and J.C. Wallmann, Bull. Am. Phys. Soc. 1, 396 (1956).

31. P. Fields, A. Friedman, B. Smaller, and W. Low, Phys. Rev. 105, 757 (1957).

32. R. Marrus, W.A. Nierenberg, and J. Winocur, Phys. Rev. 120, 1429 (1960).

33. W.A. Runciman, J. Chem. Phys. 36, 1481 (1962).

34. M. Abraham, B.R. Judd, and H.H. Wickman, Phys. Rev. 130, 611 (1963).

35. N. Edelstein and W. Easley, J. Chem. Phys. 48, 2110 (1968).

36. W. Kolbe, N. Edelstein, C.B. Finch, and M.M. Abraham, J. Chem. Phys. 56, 5432 (1972).

37. W. Kolbe, N. Edelstein, C.B. Finch, and M.M. Abraham, J. Chem. Phys. 58, 820 (1973).

38. M.M. Abraham and L.A. Boatner, Phys. Rev. B 26, 1434 (1982).

39. M.M. Abraham and L.A. Boatner, unpublished data, 1984.

40. M.M. Abraham, G.W. Clark, C.B. Finch, R.W. Reynolds, and H. Zeldes, J. Chem. Phys. 50, 2057 (1969).

41. S.A. Marei and B.B. Cunningham, J. Inorg. Nucl. Chem. 34, 1203 (1972).

42. L.R. Morss, J. Fuger, J. Goffart, and R.G. Haire, Inorg. Chem. 22, 1993 (1983).

43. B. Kanellakopulos, J.P. Charvillat, F. Maino, and W. Müller, in "Transplutonium Elements," W. Müller and R. Linder, Eds., North-Holland, Amsterdam, 1976, p. 181.

44. R.D. Baybarz, L.B. Asprey, C.E. Strouse, and E. Fukushima, J. Inorg. Nucl. Chem. 34, 3427 (1972).

45. For references to these measurements see P.G. Huray, S.E. Nave, J.R. Peterson, and R.G. Haire, Physica 102B, 217 (1980).

46. J.M. Fournier, A. Blaise, W. Müller, and J.C. Spirlet, Physica 86-88B, 30 (1977).